ISCI, Volume *21*

Supplemental Information

WRNIP1 Protects Reversed DNA Replication Forks from SLX4-Dependent Nucleolytic Cleavage

Bartlomiej Porebski, Sebastian Wild, Sandra Kummer, Sarah Scaglione, Pierre-Henri L. Gaillard, and Kerstin Gari

Supplemental Figures S1-S5

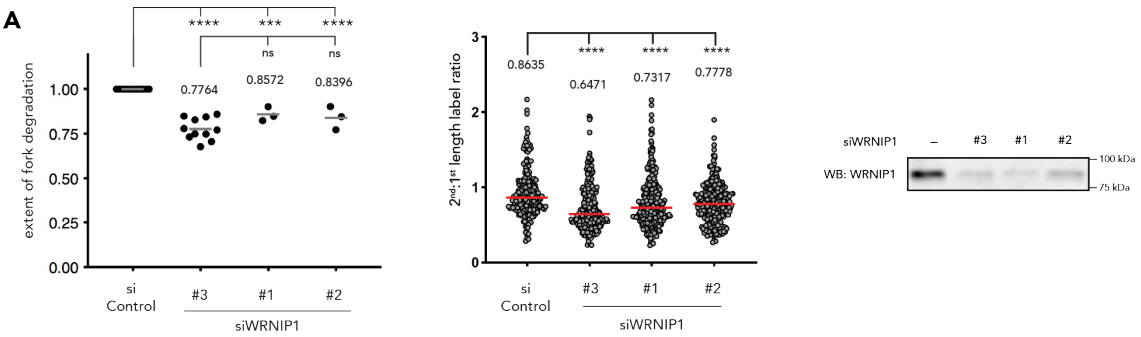

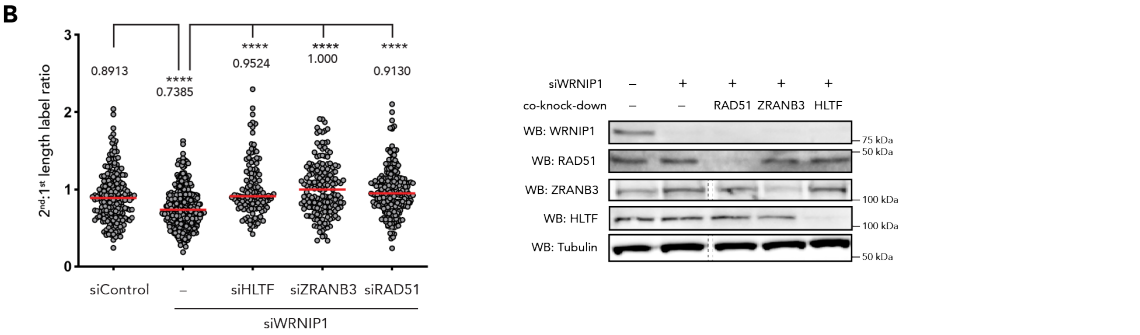

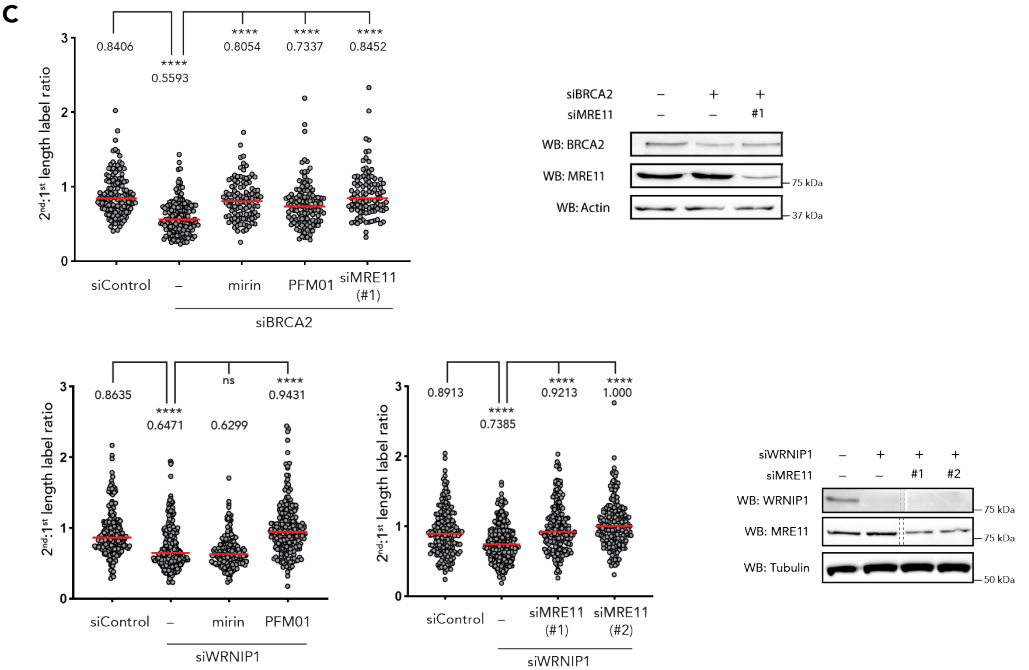

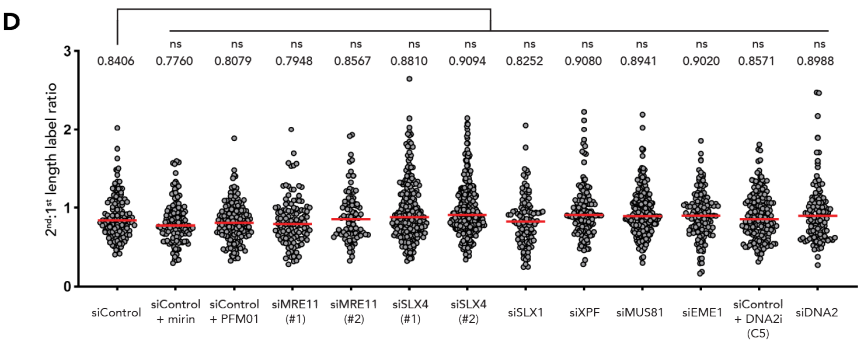

Figure S1. WRNIP1 protects reversed replication forks in a different way than BRCA2, Related to Figure 1. (A) Left: Replication fork degradation analysis in cells depleted of WRNIP1 using different siRNA sequences. Each dot represents an independent biological replicate. Values and grey bars indicate mean. Statistical analysis: one-way ANOVA with Sidak's correction for multiple comparisons. Middle: scatter plot of one representative experiment. Each dot represents one replication fork. Values and red bars indicate median. Statistical analysis: Kruskal-Wallis test. Right: western blots. (B) Replication fork degradation analysis upon knock-down of WRNIP1 and co-depletion of factors involved in replication fork reversal. Left: scatter plot of one representative experiment. Each dot represents one replication fork. Values and red bars indicate median. Statistical analysis: Kruskal-Wallis test. Right: western blots. (C) Replication fork degradation analysis upon knock-down of WRNIP1 (left) or BRCA2 (right) in the absence or presence of the MRE11 exonuclease inhibitor mirin, the MRE11 endonuclease inhibitor PFM01 or upon co-depletion of MRE11. Left: scatter plots of one representative experiment. Each dot represents one replication fork. Values and red bars indicate median. Statistical analysis: Kruskal-Wallis test. Right: western blots. (D) Replication fork degradation analysis in cells depleted of indicated nucleases or treated with indicated inhibitors. Each dot represents one replication fork. Values and grey bars indicate median. Statistical analysis: Kruskal-Wallis test. si, siRNA; WB, western blot; p values (****, $p < 0.0001$; ***, $p < 0.001$; **, $p < 0.01$; *, $p < 0.1$; ns, not significant).

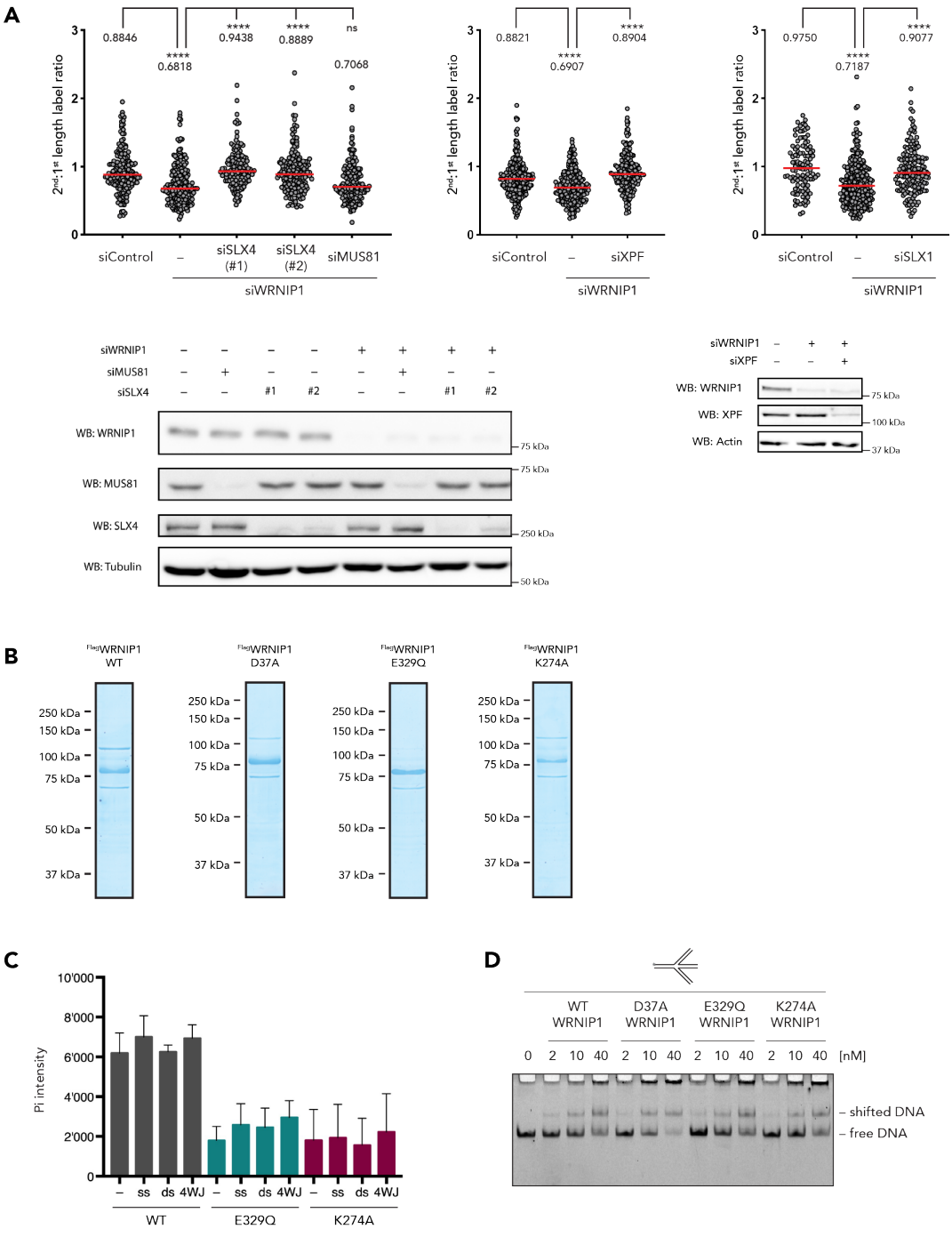

Figure S2. WRNIP1 protects reversed replication forks from SLX4-dependent nucleolytic cleavage, Related to Figure 2. (A) Replication fork degradation analysis upon knock-down of WRNIP1 and co-depletion of SLX4 and associated nucleases. Top: scatter plots of one representative experiment. Each dot represents one replication fork. Values and red bars indicate median. Statistical analysis: Kruskal-Wallis test. Bottom: western blots. (B) InstantBlue-stained SDS gels of purified Flag-WRNIP1 variants. (C) ATPase activity of wild-type WRNIP1 and the Walker A and B variants K274A and E329Q in the absence of DNA (–) or in the presence of ssDNA (ss), dsDNA (ds) or a four-way junction substrate (4WJ), as measured by release of inorganic phosphate (Pi) from radio-labelled γ-^{32}P-ATP in thin-layer chromatography. Error bars depict standard deviation from three independent experiments. (D) EMSA showing WRNIP1 variants' ability to bind to a four-way junction substrate. si, siRNA; WB, western blot; p values (****, $p < 0.0001$; ***, $p < 0.001$; **, $p < 0.01$; *, $p < 0.1$; ns, not significant).

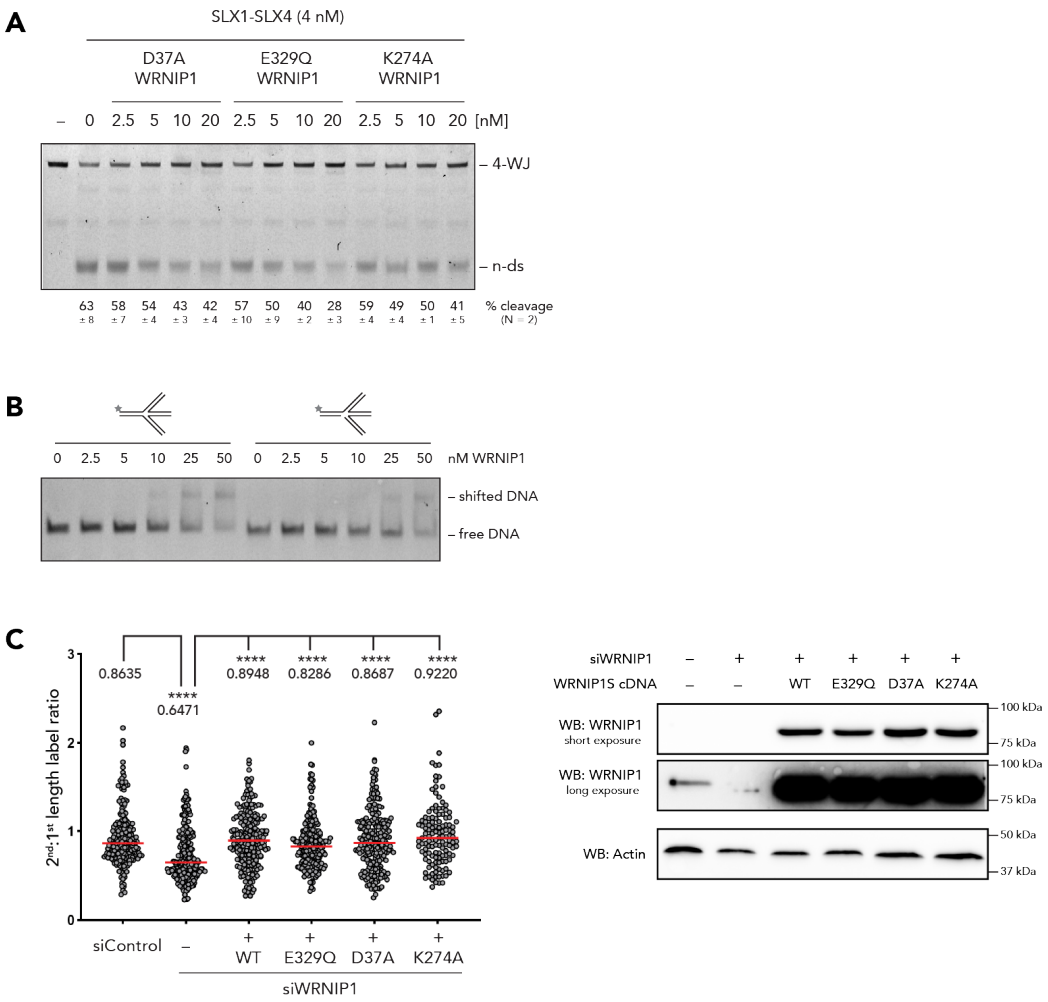

Figure S3. ATP- and ubiquitin binding are largely dispensable for WRNIP1's role at stalled DNA replication forks, Related to Figure 3. (A) Endonucleolytic cleavage assay of SLX1-SLX4 in the presence of increasing amounts of WRNIP1 variants. (B) EMSA showing binding of wild-type WRNIP1 to an intact four-way junction substrate (left) and a nicked four-way junction substrate (right). (C) Replication fork degradation analysis in WRNIP1-depleted cells, complemented with WRNIP1 variants. Endogenous WRNIP1 was depleted by siRNA targeting the 3′-UTR. Left: scatter plot of one representative experiment. Each dot represents one replication fork. Values and red bars indicate median. Statistical analysis: Kruskal-Wallis test. Right: western blots. si, siRNA; WB, western blot; p values (****, $p < 0.0001$; ***, $p < 0.001$; **, $p < 0.01$; *, $p < 0.1$; ns, not significant).

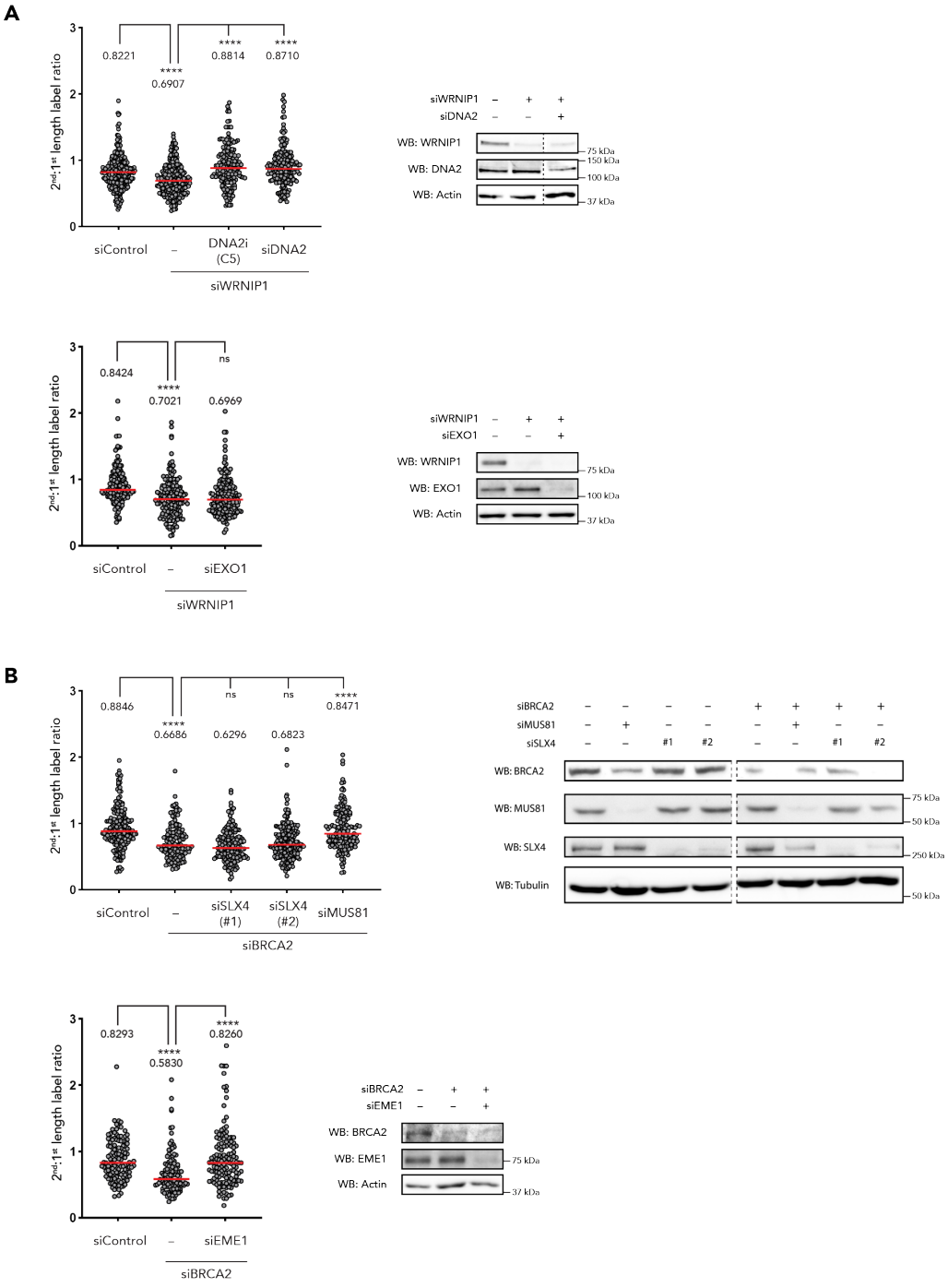

Figure S4. Fork resection requires endonucleolytic and exonucleolytic cleavage steps, Related to Figure 4. (A) Replication fork degradation analysis upon knock-down of WRNIP1 in the absence or presence of the DNA2 inhibitor C5 or upon co-depletion of DNA2 or EXO1. Left: scatter plots of one representative experiment. Each dot represents one replication fork. Values and red bars indicate median. Statistical analysis: Kruskal-Wallis test. Right: western blots. (B) Replication fork degradation analysis upon knock-down of BRCA2 and co-depletion of SLX4, MUS81 or EME1. Left: scatter plots of one representative experiment. Each dot represents one replication fork. Values and red bars indicate median. Statistical analysis: Kruskal-Wallis test. Right: western blots. Please note that the left half of the upper western blot of Figure S4B is identical to the left half of the left western blot in Figure S2A, since the experiments were done in parallel and the control samples used were the same. si, siRNA; WB, western blot; p values (****, $p < 0.0001$; ***, $p < 0.001$; **, $p < 0.01$; *, $p < 0.1$; ns, not significant).

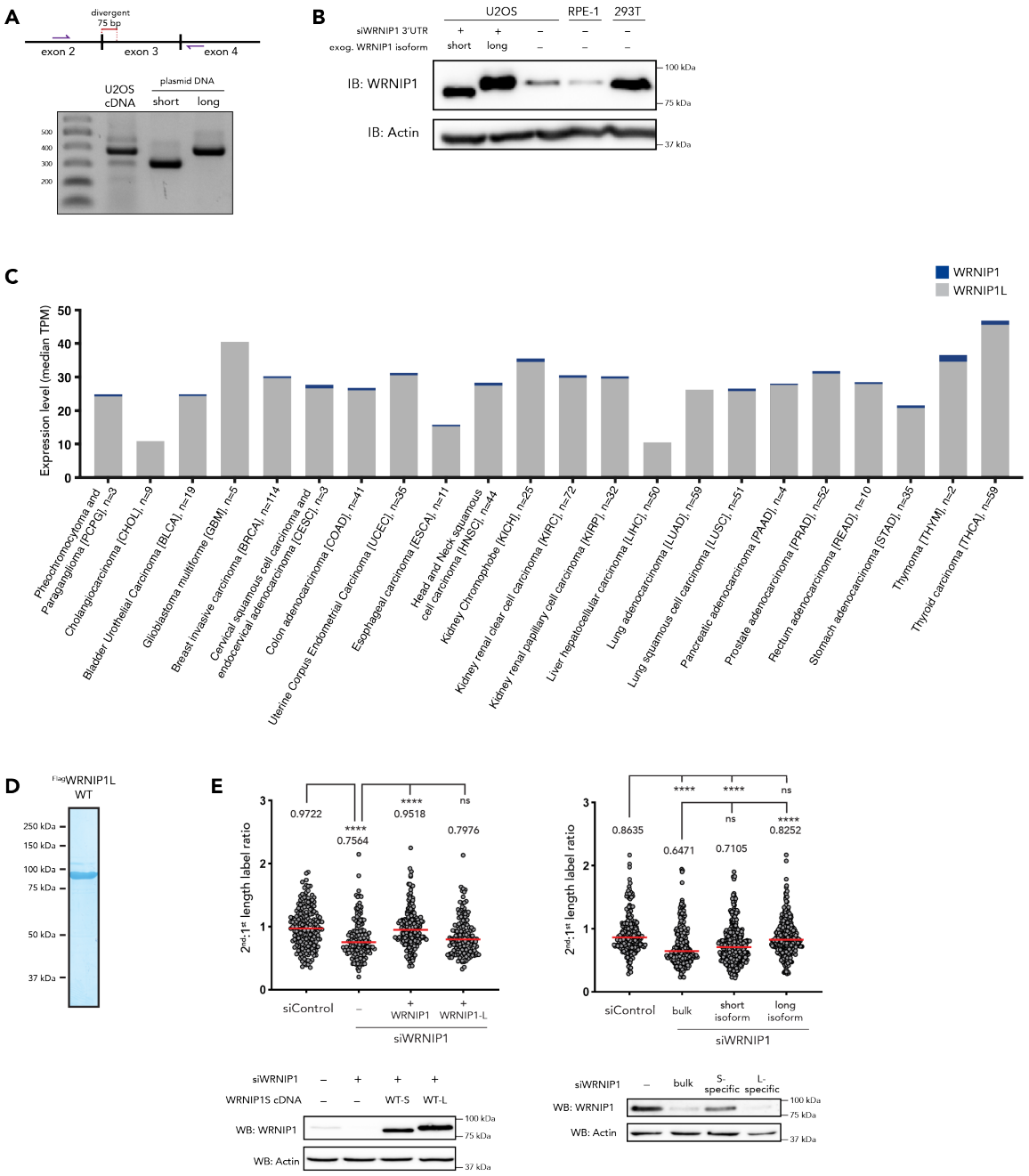

Figure S5. WRNIP1, but not WRNIP1L, can protect reversed replication forks, Related to Figure 5. (A) End-point RT PCR-based analysis of isoform abundance of WRNIP1/WRNIP1L in U2OS cells. Upper panel depicts the analysed locus. Lower panel shows electrophoretic analysis of the end-point PCR reaction on a cDNA library. (B) Western blot showing comparison of ectopically expressed untagged WRNIP1 isoforms to endogenous WRNIP1 from U2OS, RPE-1 and HEK 293T cell lines. (C) Expression levels of WRNIP1 isoforms in different tissues. Graph was generated using the ISOexpresso tool that utilises TCGA database. (D) InstantBlue-stained SDS gel of purified wild-type WRNIP1L. (E) Replication fork degradation analysis upon knock-down of WRNIP1 and complementation with cDNAs expressing the short (WRNIP1) or long (WRNIP1L) isoform (left panels). Right panels, knock-down of WRNIP1 (short isoform) or WRNIP1L (long isoform) using isoform-specific siRNAs. Top: scatter plots of one representative experiment. Each dot represents one replication fork. Values and red bars indicate median. Statistical analysis: Kruskal-Wallis test. Bottom: western blots. si, siRNA; WB, western blot; p values (****, $p < 0.0001$; ***, $p < 0.001$; **, $p < 0.01$; *, $p < 0.1$; ns, not significant).

Supplemental Tables S2-S4

Table S2. Oligos used in this study, Related to Figures 2, 3 and 5.

name	sequence (5′–3′)
X01	GACGCTGCCGAATTCTACCAGTGCCTTGCTAGGACATCTTTGCCCACCTGCAGGTTCACCC
X01c	GGGTGAACCTGCAGGTGGGCAAAGATGTCCTAGCAAGGCACTGGTAGAATTCGGCAGCGTC
X02	TGGGTGAACCTGCAGGTGGGCAAAGATGTCCATCTGTTGTAATCGTCAAGCTTTATGCCGTT
X02.1/2	TGGGTGAACCTGCAGGTGGGCAAAGATGTCC
X03	GAACGGCATAAAGCTTGACGATTACAACAGATCATGGAGCTGTCTAGAGGATCCGACTATCGA
X03.1/2	CATGGAGCTGTCTAGAGGATCCGACTATCGA
X03.1/2_2	GAACGGCATAAAGCTTGACGATTACAACAGAT
X04	ATCGATAGTCGGATCCTCTAGACAGCTCCATGTAGCAAGGCACTGGTAGAATTCGGCAGCGT

Table S3. siRNAs used in this study, Related to Figures 1-5.

name	target gene	target region	reference	sequence (5'-3')
siControl	–	–	Microsynth (neg. control)	AGG UAG UGU AAU CGC CUU G
siBRCA2	BRCA2	BRCA2 mRNA: 3401 - 3421	(Mijic et al., 2017)	AAC UGA GCA AGC CUC ACU CAA
siHLTF	HLTF	HLTF mRNA: 567 - 585	(Blastyak et al., 2010)	GGU GCU UUG GCC UAU AUC A
siMRE11 #1	MRE11	MRE11 mRNA: 2436 - 2454	this study	GAG CAU AAC UCC AUA AGU A
siMRE11 #2	MRE11	MRE11 mRNA: 1793 - 1811	(Yuan and Chen, 2010)	GGA GGU ACG UCG UUU CAG A
siMUS81	MUS81	MUS81 mRNA: 1825 - 1843	(Di Marco et al., 2017)	CAG CCC UGG UGG AUC GAU A
siRAD51	RAD51	RAD51 mRNA: 1327 - 1345	(Mijic et al., 2017)	GAC UGC CAG GAU AAA GCU U
siSLX1	SLX1	SLX1 mRNA: 1047 - 1067	(Muñoz et al., 2009)	UGG ACA GAC CUG CUG GAG AUU
siSLX4 #1	SLX4	SLX4 mRNA: 5826 - 5848	(Mutreja et al., 2018)	CGG CAU UUG AGU CUG CAG GUG AA
siSLX4 #2	SLX4	SLX4 mRNA: 3181 - 3201	(Mutreja et al., 2018)	AAA CGU GAA UGA AGC AGA AUU
siWRNIP1 #1	WRNIP1	WRNIP1 mRNA: 1099 - 1117	this study	CAA CAA AUG CCA AGA CAA A
siWRNIP1 #2	WRNIP1	WRNIP1 mRNA: 1639 - 1657	this study	CAG AGA AUG ACG UGA AGG A
siWRNIP1 #3	WRNIP1	WRNIP1 mRNA: 2301 - 2319 (3' UTR)	this study	UUA GAA CAG ACC AAC AUU U
siWRNIP1L	WRNIP1 (long isoform)	2-20 nt of the insertion	this study	ACA CUU UCC UUC CUC ACG U
siWRNIP1S	WRNIP1 (short isoform)	-4 to +14 around the insertion site	this study	CAG GUC AAC GCU GCU CUU C
siZRANB3	ZRANB3	ZRANB3 mRNA: 2127 - 2145	this study	UCA GAA AGA CAC CUC CAA A
siXPF	XPF	XPF mRNA: 341 - 359	(Mutreja et al., 2018)	GUA GGA UAC UUG UGG UUG A
siDNA2	DNA2	DNA2 mRNA: 3267 - 3285	(Thangavel et al., 2015)	CAG UAU CUC CUC UAG CUA G
siEME1	EME1	EME1 mRNA: 328 - 345	(Pepe and West, 2014)	GCU AAG CAG UGA AAG UGA A
siEXO1	EXO1	EXO1 mRNA: 2243 - 2261	(Przetocka et al., 2018)	GCC UGA GAA UAA UAU GUC U

Note that siWRNIP1 #3 was used in all experiments and is referred to as “siWRNIP1”.

Table S4. Antibodies used in this study, Related to Figures 1-5.

antibodies	manufacturer	catalogue number	source	use	dilution
primary antibodies					
WRNIP1 G-2	Santa-Cruz Biotechnology	sc-377402	mouse	WB	1:1000
WRNIP1 N-17	Santa-Cruz Biotechnology	sc-55437	goat	WB	1:1000
Flag M2	Sigma-Aldrich	F1804	mouse	WB	1:1000
His	GE Healthcare	27-4710-01	mouse	WB/IP	1:1000
HLTF	GeneTex	GTX114776	rabbit	WB	1:1000
ZRANB3	ProteinTech	23111-1-AP	rabbit	WB	1:1000
RAD51	Santa-Cruz Biotechnology	sc-8349	rabbit	WB	1:1000
MRE11	Novus Biological	NB100-142	rabbit	WB	1:1000
BRCA2	EMD Millipore	OP95	mouse	WB	1:1000
SLX4	Bethyl Laboratories	A302-270A	rabbit	WB	1:1000
MUS81	Sigma-Aldrich	M1445	mouse	WB	1:1000
XPF	Bethyl Laboratories	A301-315A	rabbit	WB	1:1000
DNA2	Abcam	ab96488	rabbit	WB	1:1000
EME1	Santa-Cruz Biotechnology	sc-53275	mouse	WB	1:1000
EXO1	Bethyl Laboratories	A302-640A	rabbit	WB	1:1000
Actin	Santa-Cruz Biotechnology	sc-47778	mouse	WB	1:2000
Tubulin	Santa-Cruz Biotechnology	sc-9104	mouse	WB	1:1000
BrdU/CldU	Abcam	ab6326	rat	DNA fibres	1:500
BrdU/IdU	Becton Dickinson	347580	mouse	DNA fibres	1:80
secondary antibodies					
anti-Mouse-HRP	Amersham	NA931	sheep	WB	1:5000
anti-Rabbit-HRP	Amersham	NA934	donkey	WB	1:5000
anti-Goat-HRP	Santa-Cruz Biotechnology	sc-2354	mouse	WB	1:5000
anti-Mouse-Alexa488	Invitrogen	A-11029	goat	DNA fibres	1:300
anti-Rat-Cy3	Jackson ImmunoResearch	712-165-153	donkey	DNA fibres	1:300

Transparent Methods

Plasmids and baculoviruses

WRNIP1 cDNA was purchased from Mammalian Gene Collection (Dharmacon) as a bacterial stab. The cDNA was cloned into pDONR221™ GATEWAY® entry vector (Invitrogen) according to the manufacturer's protocol and transformed into competent bacteria. *WRNIP1L* was cloned by a series of PCR reactions using *WRNIP1*-pDONR221 as a template. All entry vectors were analysed by restriction digest reactions and sequencing (Microsynth). GATEWAY® destination vectors were generated according to the manufacturer's protocol. Site-directed mutagenesis was performed according to the original idea of Stratagene (QuikChange® Site-Directed Mutagenesis, Stratagene) on GATEWAY® entry vectors. Bacmids and baculoviruses were generated using the Bac-to-Bac® Baculovirus Expression System (Invitrogen) approach.

Protein purifications

All human WRNIP1 variants were purified from *Sf9* insect cells. A liquid culture at a density of $2x10^6$ cells/ml was infected with baculoviruses at an MOI = 1. Cells were incubated with shaking at 25 °C for 48 hours, and harvested and lysed in 5 PCV (packed-cell volume) of Lysis Buffer (50 mM Na-phosphate pH 7.0, 150 mM NaCl, 10% glycerol, 0.1% NP-40, 1 mM TCEP, 0.5 mM EDTA), supplied with protease inhibitors cocktail (Roche) for 30 minutes on ice with intermittent vortexing. Lysates were spun down at 4 °C in a Sorvall™ WX+ (Thermo Scientific) ultracentrifuge equipped with a T-865 rotor at 37,500 rpm for 1 hour. Supernatant was collected and filtered through 0.45 µm and 0.22 µm filters. Resulting cell lysates were incubated with 0.01 volumes of equilibrated Flag M2 beads (Sigma Aldrich) for 2 hours at 4 °C with rotation. Afterwards, beads were washed 3 times for 10 minutes in 10 ml of the Lysis Buffer at 4 °C with rotation, followed by 3 washes with Storage Buffer (Lysis Buffer minus EDTA). Afterwards, bound proteins were eluted twice with 5 beads volumes of the Storage Buffer supplemented with 200 ng/µl 3x FLAG® peptide (Sigma) for 1 hour at 4 °C, with rotation. Flag-IP eluates were filtered on 0.22 µm spin columns (Bio-Rad), aliquoted, snap-frozen and stored at -80 °C. Concentration was estimated from quantification of SDS-PAGE, followed by calculations based on a BSA standard curve.

Human SLX1-SLX4 was purified from bacteria as a complex of His-tagged full-length SLX1 and the His-tagged CCD domain of SLX4, as described previously (Fekairi et al., 2009).

MUS81-EME1 was purified from bacteria, as described previously (Di Marco et al., 2017).

DNA substrates

All oligonucleotides used for DNA substrate preparation were synthesised by Microsynth and are listed in **Table S2**. Oligonucleotide X01 served as a basis for all substrates used in this study and was therefore labelled on the 5´-end by fluorescein amidite during synthesis.

Annealing of DNA substrates was done in a buffer containing 10 mM Tris-HCl pH 8.0, 50 mM NaCl and 10 mM $MgCl_2$. Oligonucleotides were mixed, incubated for 5 minutes at 95 °C and then allowed to cool down to room temperature.

DNA substrates were composed of the following oligonucleotides:

- ssDNA: X01
- dsDNA: X01, X01c
- replication fork: X01, X02.1/2, X03.1/2, X04
- 4-way junction: X01, X02, X03, X04
- nicked 4-way junction: X01, X02, X03.1/2, X03.1/2_2, X04

DNA binding

DNA binding was done in 10 µl reactions containing 1 µl of DNA substrate (final concentration: 5 nM) and 9 µl of protein dilution. Reactions were incubated on ice for 20 minutes, followed by addition of loading buffer (final: 3.5% Ficoll, 10 mM Tris-Cl pH 7.5, 10 mM EDTA, Xylene cyanol) and analysis by native gel electrophoresis using 0.5X TBE 6% polyacrylamide gels at room temperature. The gels were scanned using a Typhoon™ FLA9500 (GE Healthcare) scanner.

ATPase activity

ATPase activity was measured in 5 µl reactions containing 5 mM $MgCl_2$, 0.01 mM ATP, 0.033 µM ATP - $\gamma^{32}P$, 23.5 nM of protein and, optionally, 50 nM of a DNA substrate. Reactions were incubated at 37 °C for 30 minutes and then stopped by addition of EDTA to a final concentration of 50 mM. 1 µl of the sample was spotted on a PEI-Cellulose thin-layer chromatography plate (Merck), and the plates were resolved in a solution containing 0.15 M LiCl and 0.15 M formic acid. Resolved plates were air-dried, wrapped in cling film and analysed by autoradiography.

In vitro four-way junction protection

The reversed fork protection assay was done by titrating WRNIP1 into SLX1-SLX4 nuclease reactions. WRNIP1 was first pre-incubated with the DNA substrate (4 µl of WRNIP1 dilution, 1 µl of 50 nM DNA) for 10 minutes on ice. Then a 5 µl mix of SLX1-SLX4 in SLX reaction buffer was added to have a final concentration of 25 mM Tris-HCl pH 7.5, 0.25 mM β-mercaptoethanol, 50 µg/ml BSA (New England Biolabs), and 0.5 mM $MgCl_2$. Reactions were carried out at 37 °C for 10 minutes, deproteinised for 10 minutes at 37 °C with 2 mg/ml Proteinase K and 0.4% SDS and resolved by native PAGE through 8% polyacrylamide gels in 1x TBE. Gels were scanned using Typhoon™ FLA9500 (GE Healthcare) scanner.

Reversed fork protection assays with MUS81-EME1 were essentially done the same, except that the ME1 reaction buffer was chosen such that the final reactions contained 25 mM Tris-HCl (pH 7.5), 2.5 mM $MgCl_2$ and 20 mM KCl.

Co-IPs

The purified complex of His-tagged full-length SLX1 and the His-tagged CCD domain of SLX4 was pre-incubated with Flag-tagged WRNIP1 in lysis buffer for 1h at 4°C. In the meantime, anti-His antibodies were bound to Protein G Sepharose Fast Flow beads (Sigma Aldrich) for 2h at 4°C. The SLX1-SLX4/WRNIP1 binding mix (or the control mix containing WRNIP1 only) was then added to the beads and incubated overnight at 4°C. Beads were then washed extensively in lysis buffer and boiled in 2x sample buffer. Bound proteins were analysed by western blotting.

Mammalian cell culture

All human cell lines were grown in DMEM (Dulbecco's Modified Eagle Medium, Gibco) supplied with 10% fetal bovine serum (Gibco) at 37 °C and 5% oxygen. For replicates of phenotypical analyses, cells of similar passage number were used (±2) to ensure reproducibility of conditions. *Sf9* insect cells were grown in HyClone™ SFX-Insect™ cell culture media (GE Healthcare) at 25 °C with shaking.

Plasmid transfections

Transfection of bacmids to *Sf9* insect cells was done using TransIT®-LT1 Transfection Reagent (Mirus) according to the manufacturer's protocol. Human U2OS cells were transfected using jetPRIME® (Polyplus-transfection®) according to the manufacturer's protocol (10 µg plasmid DNA per ø10 cm culture dish; 1:3 (w/v) DNA:jetPRIME® ratio); medium was replaced after 6-8 hours.

RNA interference

Short interfering RNA duplexes were designed using Sfold (http://sfold.wadsworth.org/), unless otherwise stated, and synthesised at Microsynth. U2OS cells were transfected with siRNAs using

DharmaFECT1 Tranfection Reagent (Dharmacon). Tranfection mix equal to 1:10 of culture medium volume was prepared in Opti-MEM™ (Gibco) by mixing siRNA (final 40 nM) with the transfection reagent (0.55 µl per 100 µl of the mix, irrespective of number of siRNAs used); the mixture was incubated at RT for 10 minutes and added to the cells. The growth medium was replaced after 24 hours. Sequences of siRNAs used in the study are listed in **Table S3**.

Cell extracts

Unless otherwise stated, human and insect cells were lysed by incubating PBS-washed cell pellets with 5 PCV (packed-cell volume) of Lysis Buffer (50 mM Na-phosphate pH 7.0, 150 mM NaCl, 10% glycerol, 0.1% NP-40, 1 mM TCEP, 0.5 mM EDTA), supplied with protease inhibitors cocktail (Roche) and, optionally, 0.1% Benzonase® (Sigma) or PhosSTOP™ (Roche), for 30 minutes on ice with intermittent vortexing. Next, lysates were spun down at 17,200 x g for 30 minutes at 4 °C; supernatants were collected. If needed, concentrations of the lysates were analysed using Bradford assay and normalised.

Western blotting

For protein analysis by western blotting, samples were boiled in Laemmli sample buffer and separated by SDS-PAGE run at 180 V for 1 h or 100 V for 2 h. Proteins were then transferred onto nitrocellulose or PVDF membranes at 100 V for 1-2 hours in the cold. Afterwards, membranes were blocked in 5% milk-TBST (Tris-buffered saline supplemented with 0.01% Tween®20) solution for 30 minutes and incubated with primary antibody solution overnight at 4 °C. Then, membranes were briefly washed with TBST and incubated with appropriate secondary antibody (1:5000) for 2 hours at RT. The membranes were then washed several times with TBST and the signal was developed using Clarity™ Western ECL Blotting Substrate (Bio-Rad) or SuperSignal™ West Femto Maximum Sensitivity Substrate (Thermo Scientific).
Primary and secondary antibodies used in this study are listed in **Table S4**.

DNA fibre analysis

DNA fibre analysis was carried out following a previously published protocol (Jackson and Pombo, 1998). Prior to the analysis of DNA fibres, cells were seeded in 12-well plates at a density which ensured that the cultures were 70-80% confluent at the day of labelling. Immediately before labelling, cells were washed 3 times with pre-warmed PBS (phosphate-buffered saline). Next, cells were incubated with DMEM containing 0.04 mM CldU (5-Chloro-2´deoxyuridine, Sigma), followed by washing with pre-warmed PBS (3 times, brief). Subsequently, cells were incubated with DMEM containing 0.34 mM IdU (5´-Iodo-2´deoxyuridine, Sigma), followed by a 5 hours incubation with 4 mM hydroxyurea. Afterwards, cells were washed with PBS as previously and harvested by trypsinisation. The cells were counted, diluted to 2.5 $x10^5$ cells/ml and mixed with unlabelled cells at a 1:1 ratio. Then, 3 µl of the cell suspension was spotted onto a glass slide, 7 µl of Fibre Lysis buffer was added (200 mM Tris-Cl pH 7.4, 50 mM EDTA, 0.5% SDS in sterilised water; filtered) and the drop was pipetted up and down 5 times, avoiding drop expansion. Slides were incubated at RT for 9 minutes and tilted manually at an angle that would allow the drop to slide smoothly to the bottom in 10-15 seconds. Next, the slides were air-dried and fixed overnight in a 3:1 mix of methanol and glacial acetic acid. The slides were then washed in PBS (2 x 3 min) and DNA was denatured in 2.5 M HCl for 1 hour at RT. The slides were washed in PBS (2 x 3 min) and subsequently blocked in freshly prepared Blocking Buffer (1x PBS containing 2% Bovine serum albumin and 0.1% Tween® 20; filtered) for 40 minutes at RT. Next, 60 µl of the primary antibody mix was added on top of the slide and the slide was covered with a cover slip. The slides were incubated at RT for 2.5 hours, before cover slips were carefully removed and the slides were washed with PBST (1x PBS containing 0.2% Tween® 20; 5 x 3 min). Incubation with the secondary antibody mix and washing was done in the same way as for the primary antibody. Subsequently, the slides were air-dried in the dark, mounted with 20 µl of ProLong™ Gold Antifade Mountant

(Invitrogen), and stored at 4 °C. DNA fibres were visualised (60X objective, IX81, Olympus coupled to a CCD camera, Hammatsu) and scored using ImageJ.
For each biological replicate 100-200 replication tracts were scored, the IdU/CldU ratio was calculated for each fork, and a Kruskal-Wallis test was employed for statistical analysis within a single experiment. To correct for variations in between experiments, we then normalised the median IdU/CldU ratio for each sample to the experimental control (siControl) within an individual experiment. This value serves to describe the 'extent of fork degradation' for a single biological replicate for a given sample.
For the final analysis, the mean extent of fork degradation was determined by dividing the sum of the normalised median IdU/CldU ratios of each sample by the number of biological replicates (3 or more). While not standard in the field we decided to do this because in our view it is necessary to collect data from several independently conducted experiments and perform statistical analysis on biological replicates (individual experiments), rather than technical replicates (individual replication forks within the same sample) to assess a biological phenotype and its significance. The final statistical analysis was done using one-way ANOVA with Sidak's correction for multiple comparisons. All raw and normalised median values, the number of replication tracks scored and all *p*-values are reported in **Table S1**.

Inhibitors treatment
For the analysis of replication fork degradation with DNA fibres, mirin (Sigma Aldrich) and PFM01 (Sigma Aldrich) were added to the cells 30 minutes prior the pulse-labelling with thymidine analogues to final concentrations of 50 and 10 μM, respectively, and kept throughout the labelling and hydroxyurea treatment. The DNA2 inhibitor C5 (Aobious Inc.) was used at a final concentration of 20 μM and was added together with hydroxyurea.

RT-PCR
For WRNIP1 mRNA analysis, total RNA was extracted from U2OS cells using RNeasy Mini Kit (Qiagen). Then, cDNA synthesis was done using the High Capacity RNA-to-cDNA Kit (Applied Biosystems) according to the manufacturer's protocol, followed by end-point PCR with WRNIP1-specific primers.

WRNIP1 sequence alignment
Primary sequence alignment was done using Clustal Omega algorithm, accessed through the Uniprot website (www.uniprot.org). Accession numbers of aligned proteins were: Q96S55-2 (*H. sapiens*), Q96S55-1 (*H. sapiens*), Q91XU0 (*M. musculus*), Q75JU2 (*D. discoideum*), P40151 (*S. cerevisiae*), O13984 (*S. pombe*) and P0AAZ4 (*E. coli*).

References

Blastyak, A., Hajdu, I., Unk, I., and Haracska, L. (2010). Role of Double-Stranded DNA Translocase Activity of Human HLTF in Replication of Damaged DNA. Mol. Cell. Biol. 30, 684–693.

Fekairi, S., Scaglione, S., Chahwan, C., Taylor, E.R., Tissier, A., Coulon, S., Dong, M.Q., Ruse, C., Yates, J.R., Russell, P., et al. (2009). Human SLX4 Is a Holliday Junction Resolvase Subunit that Binds Multiple DNA Repair/Recombination Endonucleases. Cell 138, 78–89.

Jackson, D.A., and Pombo, A. (1998). Replicon clusters are stable units of chromosome structure: Evidence that nuclear organization contributes to the efficient activation and propagation of S phase in human cells. J. Cell Biol. 140, 1285–1295.

Di Marco, S., Hasanova, Z., Kanagaraj, R., Chappidi, N., Altmannova, V., Menon, S., Sedlackova, H., Langhoff, J., Surendranath, K., Hühn, D., et al. (2017). RECQ5 Helicase Cooperates with MUS81 Endonuclease in Processing Stalled Replication Forks at Common Fragile Sites during Mitosis. Mol. Cell 66, 658-671.e8.

Mijic, S., Zellweger, R., Chappidi, N., Berti, M., Jacobs, K., Mutreja, K., Ursich, S., Ray Chaudhuri, A., Nussenzweig, A., Janscak, P., et al. (2017). Replication fork reversal triggers fork degradation in BRCA2-defective cells. Nat. Commun. 8, 859.

Muñoz, I.M., Hain, K., Déclais, A.C., Gardiner, M., Toh, G.W., Sanchez-Pulido, L., Heuckmann, J.M., Toth, R., Macartney, T., Eppink, B., et al. (2009). Coordination of Structure-Specific Nucleases by Human SLX4/BTBD12 Is Required for DNA Repair. Mol. Cell 35, 116–127.

Mutreja, K., Krietsch, J., Hess, J., Ursich, S., Berti, M., Roessler, F.K., Zellweger, R., Patra, M., Gasser, G., and Lopes, M. (2018). ATR-Mediated Global Fork Slowing and Reversal Assist Fork Traverse and Prevent Chromosomal Breakage at DNA Interstrand Cross-Links. Cell Rep. 24, 2629--2642.e5.

Pepe, A., and West, S.C. (2014). MUS81-EME2 Promotes Replication Fork Restart. Cell Rep. 7, 1048 1055.

Przetocka, S., Porro, A., Bolck, H.A., Walker, C., Lezaja, A., Trenner, A., von Aesch, C., Himmels, S.F., D'Andrea, A.D., Ceccaldi, R., et al. (2018). CtIP-Mediated Fork Protection Synergizes with BRCA1 to Suppress Genomic Instability upon DNA Replication Stress. Mol. Cell 72, 568-582.e6.

Thangavel, S., Berti, M., Levikova, M., Pinto, C., Gomathinayagam, S., Vujanovic, M., Zellweger, R., Moore, H., Lee, E.H., Hendrickson, E.A., et al. (2015). DNA2 drives processing and restart of reversed replication forks in human cells. J. Cell Biol. 208, 545–562.

Yuan, J., and Chen, J. (2010). MRE11-RAD50-NBS1 complex dictates DNA repair independent of H2AX. J. Biol. Chem. 285, 1097–1104.